Shear behaviour of architectural fabrics subjected to biaxial tensile loads

A.G. Colman[1], B.N. Bridgens[1♣], P.D. Gosling[1], G-T. Jou[2], X-Y. Hsu[2]

[1] School of Civil Engineering & Geosciences, Newcastle University, Newcastle-upon-Tyne, NE1 7RU, UK.

[2] Taiwan Textile Research Institute, 6 Chengtian Rd., Tucheng District, New Taipei City 236, Taiwan, R.O.C.

♣ Corresponding author: ben.bridgens@ncl.ac.uk; +44(0)191 208 6409

Keywords: A. Fabrics/textiles; B. Mechanical properties; D. Mechanical testing

Abstract

Broad assumptions are made in the testing and simulation of architectural fabrics used for tensile fabric structures. In particular, fabric shear behaviour is poorly understood and is not routinely determined. Tensile structures are continuously subject to a combination of biaxial tensile stress and shear stress, yet there is no accepted method for accurately determining shear behaviour in a tensioned fabric. A novel picture frame shear test design and associated test protocol is described here that aims to provide a practicable solution for the accurate determination of the in-situ shear stiffness of architectural fabrics. Results of shear tests on fabrics subjected to increasing levels of biaxial prestress are presented and the implications for analysis are discussed.

1 Introduction

1.1 Tensile fabric structures

Twenty years ago it was common practice to neglect the influence of shear in architectural fabrics when analysing tensile fabric structures [1] . Shear behaviour remains absent from some analysis methodologies used by industry [2]. Where shear stiffness is considered, the available guidance advises rule-of-thumb estimates [3] despite it being known that shear stiffness can impact significantly on the analysis results [3, 4].

Tensile fabric structures have been used in state-of-the-art buildings (Fig.1) for over forty years [5], including airports, sports stadia, shopping centres and large enclosed public spaces. All imposed loads are resisted by in-plane tensile and shear stresses by virtue of the structure's anticlastic (doubly curved) surface shape, applied pretension and large deflection behaviour [6].

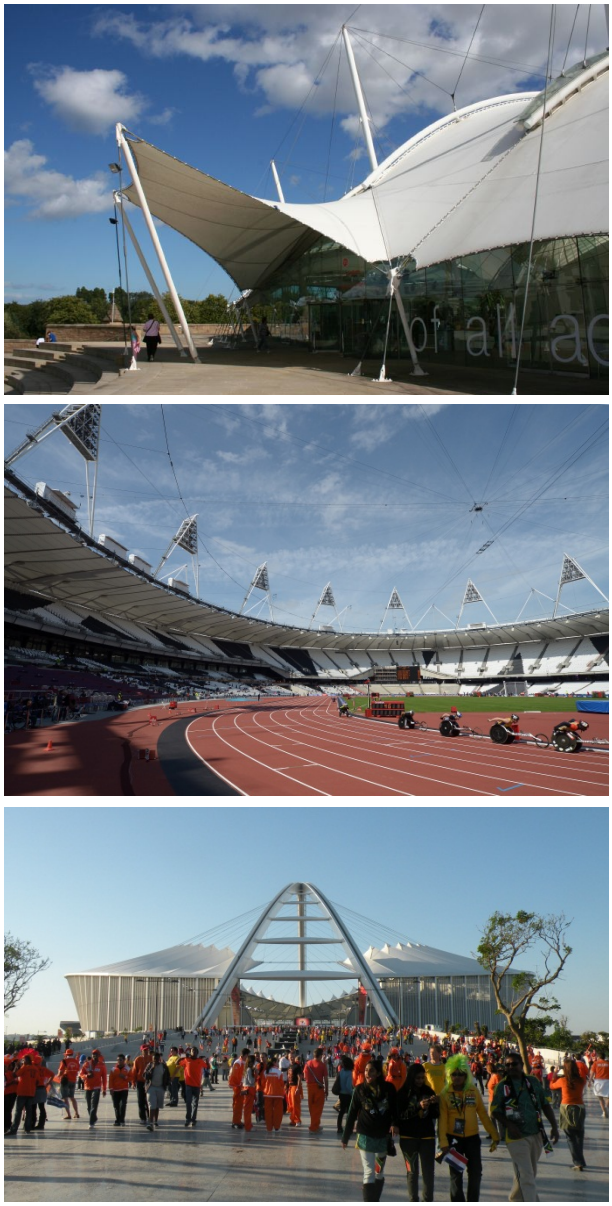

Fig. 1. (From top to bottom) Dynamic Earth Centre, Edinburgh ©Ben Bridgens; 2012 Olympic Stadium, London ©London 2012; and Moses Mabhida Stadium, Durban ©Schlaich Bergermann und Partner/Knut Göppert

Understanding and quantifying shear behaviour of architectural fabrics is important to designers, as large shear deformations are inherent in tensile fabric structures, both during installation and under imposed loading. As pretension is applied during installation, flat panels of fabric must undergo shear deformation to achieve the required smoothly curved anticlastic form. Shearing of the fabric will also occur due to large deflections in response to wind pressure and snow load. Furthermore, it is asserted that woven materials have a limiting shear deformation after which wrinkling will occur [7]. Wrinkling is unacceptable, both aesthetically if it occurs during installation, and as a potential

cause of failure if it occurs under imposed loading. Despite this, neither the shear deformations that occur in membrane structures, nor the values of limiting shear angle for particular fabrics, have been quantified.

Accurate determination of shear stiffness will allow for the improved prediction of deflection and formability of tensile fabric structures as well as avoidance of wrinkling. Therefore, safer and more efficient structural solutions will be possible and designers will be able to explore more innovative architectural forms.

1.2 Architectural fabrics

Architectural fabrics are composite materials that generally comprise a base cloth of plain woven yarns encased in a polymeric coating. Coatings protect the base cloth from damage, provide stability to the weave pattern and make the fabrics impermeable to water. Predominant material combinations are polyvinylchloride (PVC) coated polyester yarns and polytetrafluoroethylene (PTFE) or silicone coated glass-fibre yarns. The combination of two different materials and the woven yarn structure of the base cloths results in complex in-plane tensile and shear behaviour. Crimp interchange (the interaction between the woven yarns) results in non-linear biaxial stress-strain behaviour that is both hysteretic and anisotropic [8]. Elastic moduli, Poisson's ratios and shear stiffness are not constrained by the same relationships as for homogeneous, isotropic materials and elastic constants are arguably inappropriate for describing the complex mechanical behaviour of coated woven fabrics [9]. The mechanical properties of architectural fabrics are not proportional to their thickness, and it is standard practice to define stiffness values in 'kN/m width' with no reference to the fabric thickness [10].

The shear stiffness of architectural fabrics is predominantly governed by the protective polymeric coating [11] and is routinely assumed to be linear [2, 4, 12]. It is important to distinguish between shear of fabrics with and without yarn rotation. Typically, shear of woven fabrics refers to a change in angle between perpendicular yarn sets. However, shear can also occur with no change in angle between perpendicular yarn directions. The latter circumstance is observed when strain occurs in the perpendicular yarn directions and the strain in one direction does not equal that in the other. Fig. 2a shows 15° of shear deformation with yarn rotation and Fig. 2b shows 15° of shear deformation without yarn rotation. When this happens, shear resistance mechanisms of the coating are mobilised and the biaxial and shear behaviours will be linked. This paper is concerned with shear deformation that results in a change in angle between the yarns, as it is this type of shear deformation that is required to develop a curved surface from flat panels during installation. Note also that shear of

woven fabrics is pure shear (Fig. 2c) with constant side lengths, as opposed to simple or 'engineering' shear (Fig 2d) which maintains a constant area.

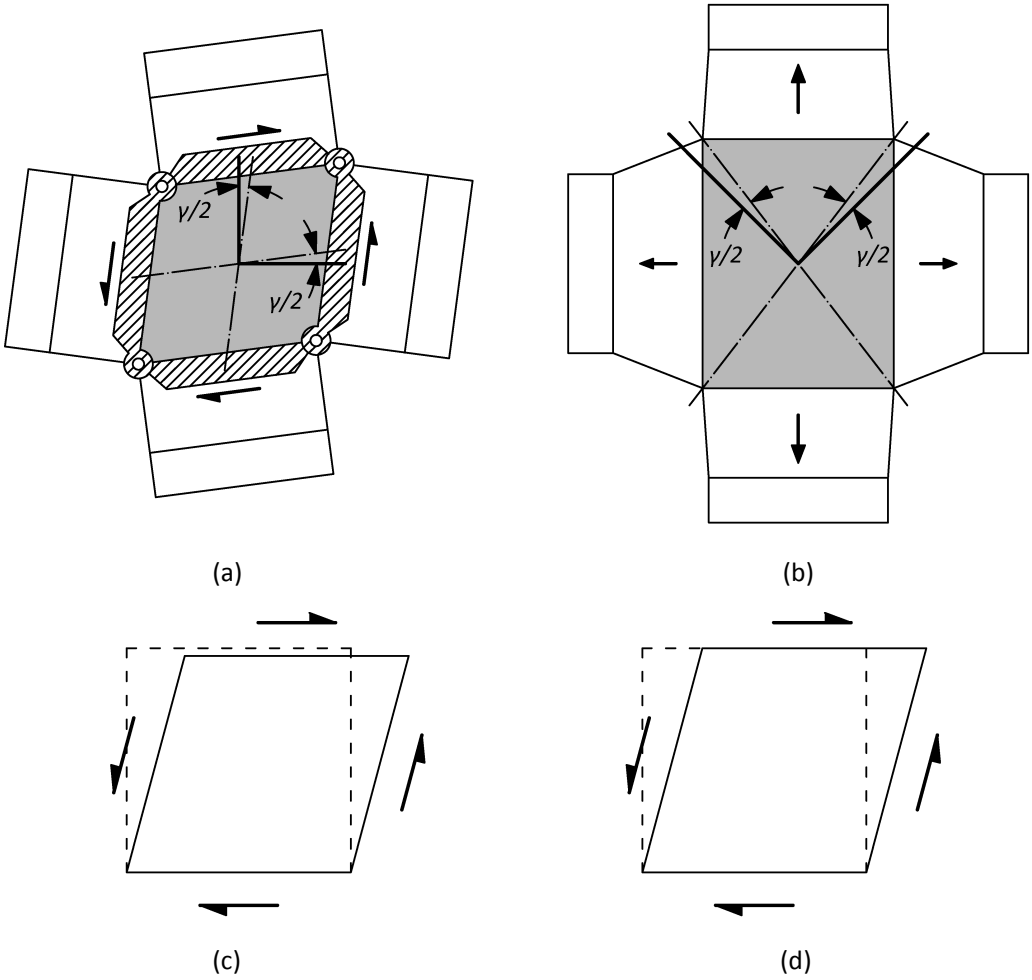

Fig. 2. Shear of architectural fabrics. (a) Shear of biaxial specimen with yarn rotation; (b) shear of biaxial specimen without yarn rotation, (c) pure shear, where area reduces but yarn length stays constant; (d) simple shear, where constant area but yarns extend

1.3 Shear testing

The only standardised methodology for the shear characterisation of architectural fabrics has been produced by the Membrane Structures Association of Japan [13]. Therefore, further development of test equipment and methodologies must look to this standard, previously published experimental works, and industry best practice. Much of the available literature related to shear testing of fabrics concerns uncoated fabrics for use in composite forming [14-21]. This work is useful in the development of methodologies for the testing of architectural fabrics, but it is important to recognise that key differences exist when considering shear of *coated* fabrics. Uncoated fabrics are

typically tested to large angles of shear and have low shear stiffness, compared to architectural fabrics that are tested at smaller angles and have relatively high shear stiffness (Table 1).

Table 1
Review of maximum angles of shear deformation and approximated linear shear stiffness for uncoated and coated fabrics

	Year	Authors	Test methodology	Max. γ (°)	G (kN/m)
Uncoated studies	2000	Page and Wang [19]	Bias extension	55	0.005*
	2007	Zhu et al. [17]	Bias extension	50	0.01*†
	2008	Launay et al. [15]	Picture frame and bias extension	50	0.23-1.09*
	2008	Cao et al. [14]	Picture frame and bias extension	55	0.04-0.09*
Coated studies	2005	Vysochina et al. [22]	T-shaped specimen	15	50.4 and 51.5
	2008	Bögner-Balz and Blum [23]	45° biaxial cruciform	15	1.3-2.4
	2009	Jackson et al. [24]	Picture frame	15	5.0-143.2
	2012	Galliot and Luchsigner [25]	Shear Ramp	15	8.9-57.8

* Approximate linear stiffness to 15°
† Calculated with use using the method proposed in [15] from crosshead load

Methodologies for shear testing of woven materials have been described by Galliot and Luchsinger [26]. To accurately simulate the *in situ* behaviour of an architectural fabric it is necessary to simultaneously apply predetermined biaxial tension and shear deformation. Furthermore, it is desirable to apply a homogenous strain field to the fabric specimen as this allows simple calculation of the stresses resulting from the applied load. Assumptions regarding homogeneity of strain fields in during shear deformation must be validated [16]. The KES-F shear test [27, 28], T-shaped specimen test [22] and extensively used bias extension test [14-18, 21] cannot apply biaxial tension whilst shearing the specimen. The biaxial cruciform test with 45° yarns [23, 29] applies biaxial tension, but the level of tension varies with shear deformation, and cannot be independently controlled. This method also requires a specimen that is difficult to prepare and can only apply 1:1 biaxial stress ratios. The inflated cylinder test [30] does allow independent control of biaxial tension and shear (through axial tension, inflation pressure and torsion, respectively), but no procedure to quantify the influence of the seam is presented. Galliot and Luchsinger [25, 26] have developed an alternative methodology, the 'shear ramp', which produces a non-homogeneous shear strain field and consequently a non-homogeneous shear stress field. Therefore, the complex calculation of a correction factor is required to analyse the test results. Recently, Harrison *et al.* [31] developed a biaxially stressed bias test, by applying a load to each side of a bias test specimen by means of an arrangement of clamps and weights. However, in its present form the approach cannot control the

load applied by the weights and no assessment of homogeneity of the strain field has been undertaken.

The picture frame shear test [14, 15, 18, 21, 32-36] allows application of biaxial prestress, which, subject to stress relaxation, can be maintained during a subsequent shear test by clamping the shear specimen along its edges. The frame subjects the specimen to a uniform deformation that should result in a homogenous state of pure shear. Homogenous deformation allows for calculation of the shear stress-strain relationship and definition of the shear stiffness. A further benefit of this method is that the fabric can be biaxially mechanically conditioned [8] prior to shear testing, to enable medium to long term fabric behaviour to be explored. For these reasons this test method has been adopted for this research.

2 Picture frame design

A number of different picture frame designs currently exist and frame and specimen dimensions vary between laboratories [14]. All designs have common features, including pinned corner connections and clamping mechanisms to secure the specimens. Typical practice is to mount specimens such that the material is clear of a frame's pinned corner connections (Fig. 3a). This prevents localised buckling of the specimen and disruption to the stress field. However, removing the corners is undesirable as it requires the arms and fingers of the sample (which are only subject to uniaxial stress) to transfer shear from the frame to the centre of the specimen [16]. This can result in a high level of 'lag' between the shear angle of the frame and the shear deformation of the test specimen. (Fig. 3b). Alternatively, the specimen can be fitted such that it fills the frame, though with material removed around the hinged corner connections (Fig. 3c). Lomov et al. [16] demonstrated that in this configuration the bending of the yarns near to the clamped edge impacts on the shear angle transferred from the frame into the specimen. However, yarn dimensions of architectural fabrics are smaller and the shear stiffnesses are higher when compared with the fabrics used in the aforementioned work. Therefore, it is anticipated that this effect will be negligible, though nevertheless deformation will be examined for this possible occurrence.

Two previous studies [24, 35] used picture frames that allowed for specimen to be fitted such that they completely fill the frame, with no material removed in the corners. However, these frame designs that allow the specimen to be 'fully fitted' fail to correctly consider the kinematics of the frame; the centre of the pinned corner connections (about which the frame hinges) are not aligned with the clamped edges of the specimen. This causes a 'scissor effect' resulting in loss of biaxial stress across the specimen and local buckling in the corners of the frame. To achieve the desired

homogenous shear strain, and therefore allow accurate calculation of shear stress, the centre of the pinned connections must align with the clamped edges of the specimen, as described by Bassett and Postle [20] (Fig. 4). However, Bassett and Postle did not develop a practical implementation of their frame design capable of fully fitting a specimen with correct alignment of the hinges.

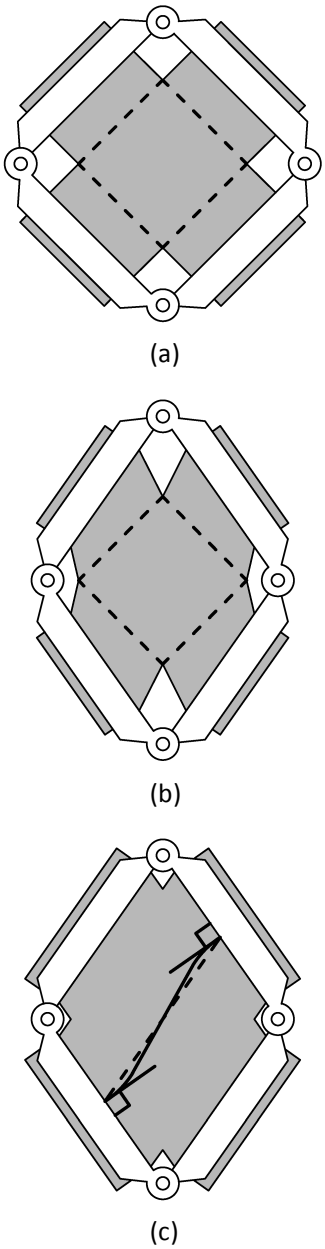

Fig. 3. Picture frame set-up; (a) undeformed picture frame with fabric cut away from the corners; (b) deformed picture frame showing retarded biaxial shear deformation; and (c) deformed picture frame with specimen more tightly fitted in frame

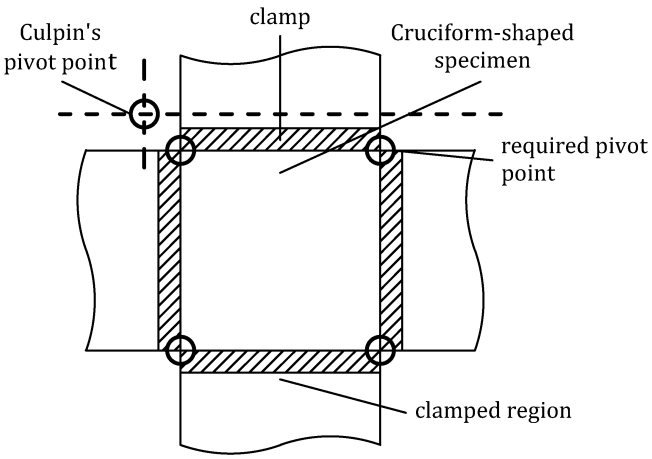

Fig. 4. The requirement for a pivot point aligned with the corner of the specimen was identified by Basset and Postle (reproduced from [20])

The proposed frame design does not require removal of material from the specimen at the corners, enabling optimum transfer of biaxial and shear force from the frame to the test specimen, whilst maintaining correct positioning of the pinned connections. The novel design achieves this whilst allowing free yarn rotation in the corners of the specimen, as the pinned connections do not penetrate the plane of the fabric. The frame (Fig. 5) comprises four pairs of aluminium bars with a machined, serrated steel grip inlayed into each bar. A yoke provides the hinge at each of the frame's corners and enables the pinned connections to align with the edge of frame. The steels grips protrude slightly from the aluminium bars allowing the pairs of bars to be correctly secured without compressing the specimen at the connections (where the yarns must be free to rotate). The grips are also machined to fit around the yokes to provide an area behind the pin to secure the specimen along its entire width. As the pins cannot pass through the plane of the fabric, each corner has a front and rear pin. The front and rear pins are aligned at the top and bottom corners of the frame by means of a bracket used to connect the frame to a uniaxial test machine (Fig. 5c). This two-part bracket connected with shoulder bolts ensures that the centres of all of the yokes align. Alignment is ensured with a bracket at only two opposing corners of the frame (Fig. 5b) and small lugs are used to pin the connections at the remaining two corners. The frame is designed for a 300x300mm biaxial cruciform specimen. Frames of other dimensions could take the same form.

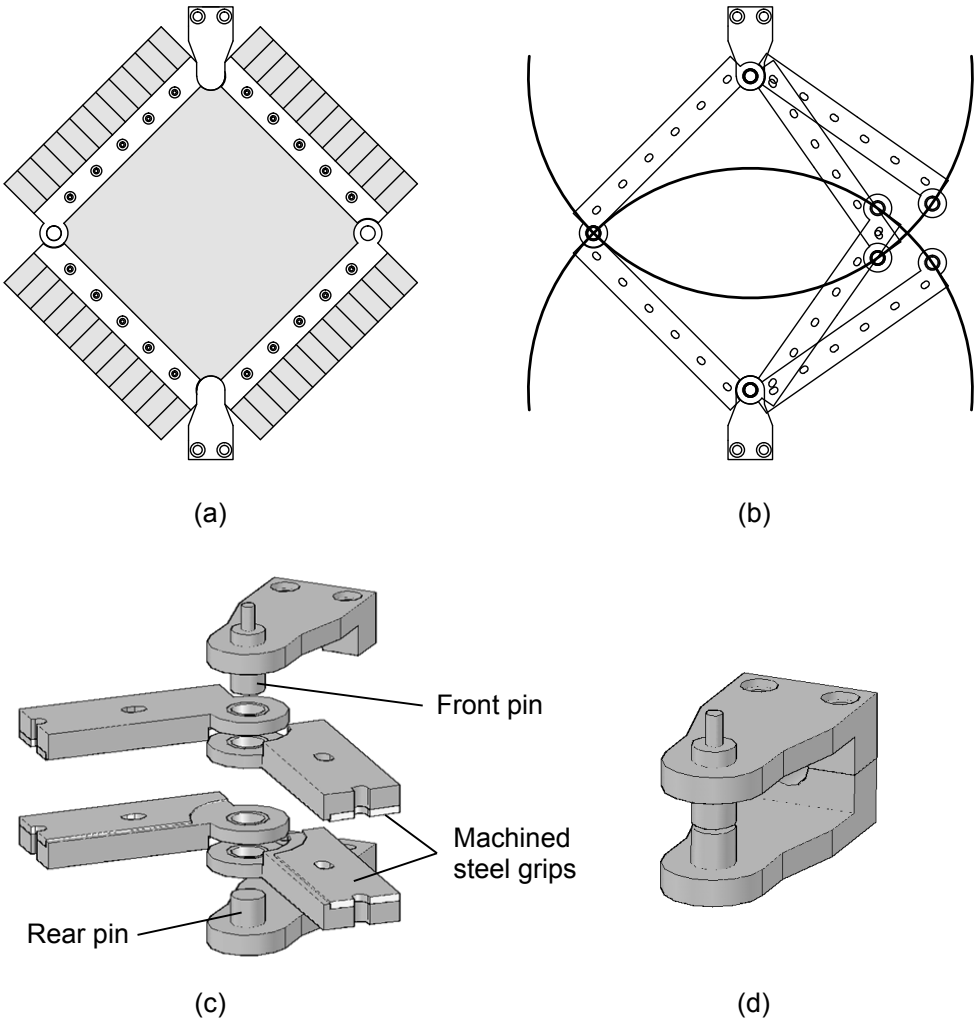

Fig. 5. (a) Schematic of picture frame shear tester developed; (b) alignment of the frame's components; (c) exploded view of pinned corner connection; and (d) aligned corner bracket

3 Experimental procedure

3.1 Shear testing

Three plain-woven architectural fabrics were used to investigate the influence of biaxial stress on fabric shear behaviour (Table 2). These fabrics were chosen to represent a range of strengths, shear stiffnesses and constituent materials. Biaxial stresses of 3%, 6% and 9% of each fabric's ultimate tensile strength were applied prior to, and maintained during, shear testing (Table 3). 3% of ultimate tensile strength corresponds to a typical prestress value, with 6% and 9% values being used to

explore how the shear behaviour varies with increasing biaxial stress. Shear behaviour at other biaxial stress ratios would also be of interest, but was beyond the scope of this work.

Table 2.
Test materials

Fabric	Manufacturer	Material		Weight (g/m^2)	Thickness (mm)	Tensile strength* (kN/m)
		Base cloth	Coating			
SCC200	Taiyo Kogyo, Japan	PET	PVC	832	0.68	76/81
CMX220	Taiyo Kogyo, Japan	Glass fibre	PVC	813	0.55	115/111
FGT1000	Chukoh, Japan	Glass fibre	PTFE	1700	1.00	207/177

*as specified by the manufacturer (warp direction/fill direction)
PET = Polyethylene terephthalate; PVC = Polyvinylchloride; PTFE = Polytetrafluoroethylene

Table 3.
Prestress applied to specimens

Fabric	% UTS	Prestress (kN/m) Warp/FIll
SCC200	3	2.25 x 2.43
	6	4.50 x 4.86
	9	6.75 x 7.29
CMX220	3	3.45 x 3.33
	6	6.90 x 6.66
	9	10.32 x 9.99
FGT1000	3	6.18 x 5.31
	6	12.36 x 10.72
	9	18.54 x 15.93

3.2 Sample preparation and test protocol

A fabric cruciform is cut with the arms parallel to the yarn directions [37] (Fig. 6). This preparation method enables the biaxial stress to be correctly applied to the yarns; load is resisted in-line with the yarns without inducing undesired shear deformation. A 'floating' biaxial test rig [37] is used to apply and maintain biaxial pretension in each specimen for a period of one hour. After this time the rate of creep of the fabric is very low, even for polymeric materials such as PVC coated polyester. Subsequently, the shear frame is fitted around the specimen with the bars of the frame parallel to the yarn directions. The biaxial test rig maintains the level of biaxial stress during the fitting of the shear test frame. Tightening of the bolts that penetrate the bars and arms of the fabric specimen

holds the applied pretension in the fabric, which allows the test specimen and shear frame to be removed from the biaxial test rig and placed in a uniaxial test machine for shearing. A cyclic shear test profile was then applied to each of the specimens (Fig. 7). The shear test profile comprises a positive and negative half of each shear cycle, where the frame is extended and compressed in the axis of the uniaxial test rig, respectively. The rate of applied cross-head displacement was 2mm/min, which is equivalent to a frame rotation rate of between 0.5 and 0.6 °/min, depending on the angle of deformation and the direction of movement.

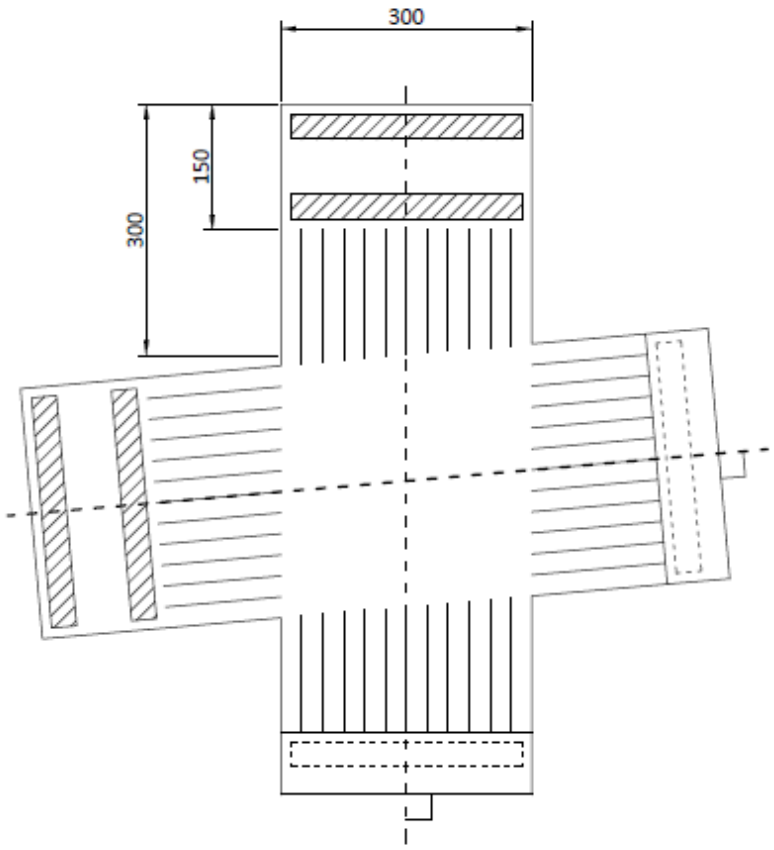

Fig. 6. Cruciform biaxial specimen prepared with arms parallel to the yarn directions (angle between warp and fill is exaggerated) [37]. Centreline dimensions are the same for each arm. Top and left arms are un-bonded; bottom and right arms show pockets formed by folding and bonding the specimen to itself.

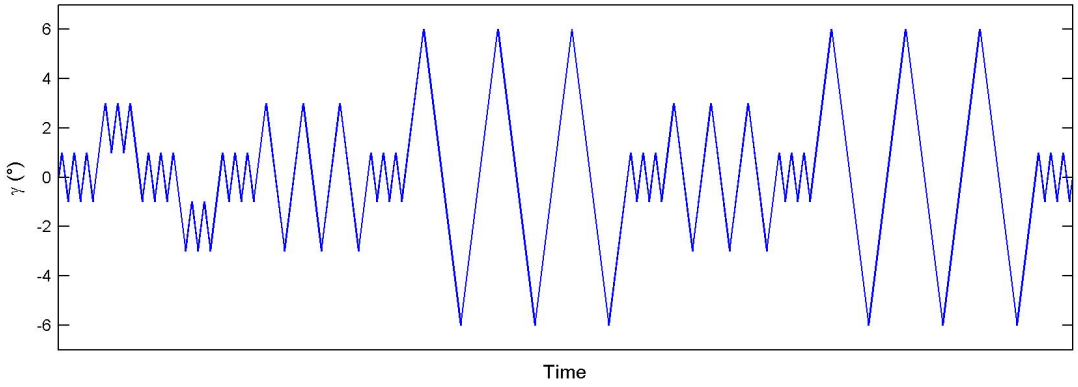

Fig. 7. Cyclic shear test profile used in the study; 13 cycle sets include shear deformation of 1°, 3° and 5°. Repeated angles allow investigation of possible softening/stiffening and were performed at a rate 2mm/mm of crosshead displacement

3.3 Determination of shear stress and strain

Shear force, F_s, applied to the fabric is resolved from the crosshead load of the uniaxial test machine (Eq. 1), where P is the crosshead load, α is the initial inside angle of the frame (typically 90°, but can vary if the fabric is non-orthogonal), γ is the shear angle, and L is the side length of the test specimen.

$$F_s = \frac{P}{2 \times \cos\left(\frac{\alpha - \gamma}{2}\right) \times L}$$

(Equation 1)

Deformation measurements obtained from an arrangement of three contact linear extensometers are used to calculate an estimate of the strains in the directions of the yarns and the shear strain (Fig. 8). The extensometers are affixed to the test specimen by aluminium mounts, comprising a 2mm threaded bar that penetrates the fabric and Ø25mm discs which hold the mount perpendicular to the plane of the fabric. A similar approach was used by Galliot and Luchsinger [25], but the formulation here allows for initially non-orthogonal yarns. Such an approach offers a straightforward method that can easily be set-up on each specimen.

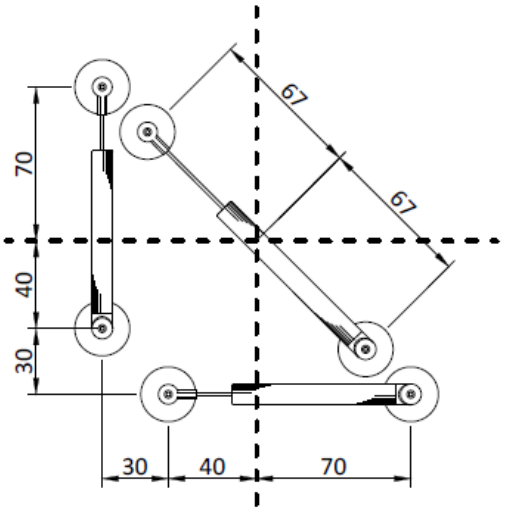

Fig. 8. Schematic of triangular arrangement of contact extensometers, dotted lines indicate specimen centrelines

To assess the suitability of the use of linear extensometers to measure shear deformation, and to assess the overall suitability of the picture frame design and test method, a Digital Image Correlation (DIC) technique was used. DIC is an optical technique for measuring deformation of an object's surface, and that has been used to assess the homogeneity of strain fields in previous textile deformability studies [16, 17, 25] through the full-field strain measurement of the entire specimen. DIC is a non-contact measurement solution and does not alter the stiffness of a material under inspection. Strains are calculated from images of the deformed specimen, is covered in a stochastic pattern (Fig. 9). Commercially available software (*Correlated Solutions' Vic-Snap* and *Vic-3D, www.correlatedsolutions.com*) is used to capture and process images from two cameras to measure deformation in three dimensions, from which a two-dimensional strain field may by derived. Images were recorded at 30-second intervals during the test and a modified profile was used which includes higher shear angles to assess the limitations of the shear frame.

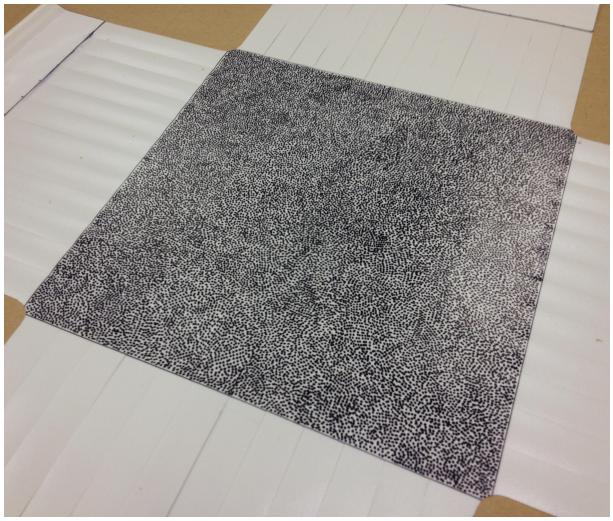

Fig. 9. Biaxial cruciform specimen (CMX220) prepared for shear test with stochastic speckle pattern for Digital Image Correlation (DIC) analysis. The pattern has been applied to the specimen with a permanent marker pen, whilst time consuming this provides a higher quality speckle pattern than spray painting or other methods, and hence a more accurate measurement of the strain field.

4 Results and Discussion

4.1 Strain field homogeneity

From visual observations made during the shear testing, no out-of-plane deformation is induced by the frame design. Yarns are free to rotate, thus preventing wrinkling at the corners unlike in previous frame designs (Fig. 10). These observations were supported by the out-of-place displacements recorded by the DIC. The shear strain results obtained from DIC analysis show that the shear deformation is not absolutely uniform across the sample (Figs. 11 and 12). However, the variation is small - standard deviations of the shear strain across the entire sample do not exceed 5% of the average shear strain (Table 4) – so the shear deformation can be considered to be homogeneous. The 5% criterion is based on a previous study [25], in which it was only valid for a small central area of the specimen. Here it is true across the entire specimen for each of the angles prescribed up to the maximum, $\gamma = 15°$. The variation is likely to be the result of bending of the yarns near to the clamped edge, as described previously. The DIC results also show agreement with the shear angles calculated from extensometer readings (Fig. 12) and thus the extensometers provided a suitable means to obtain the shear deformation of the specimen during testing. Whilst the shear strain can be considered to be homogeneous across the specimen, the shear strain induced in the specimen is less than the shear angle of the frame, again due to yarn rotation at the clamps. This is not problematic if the shear strain is calculated from extensometer readings, but it does mean that crosshead movement cannot be used as an accurate measure of shear strain.

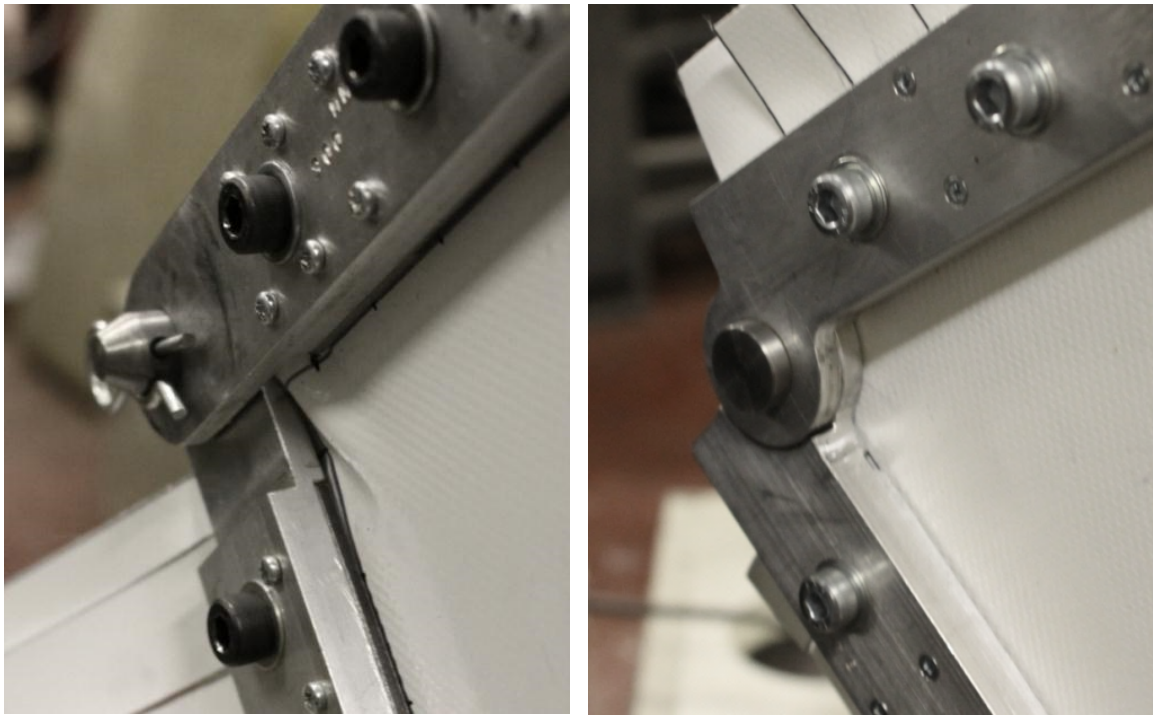

Fig. 10. (a) Picture frame used by Jackson et al. [24] showing localised buckling of the specimen in the corners of the frame due to the pivot point being offset from the corner of the specimen and no clamping behind the corners, γ = 15°; and (b) New picture frame design showing no frame induced buckling, γ = 15°. Reproduced after Colman et al. [38]

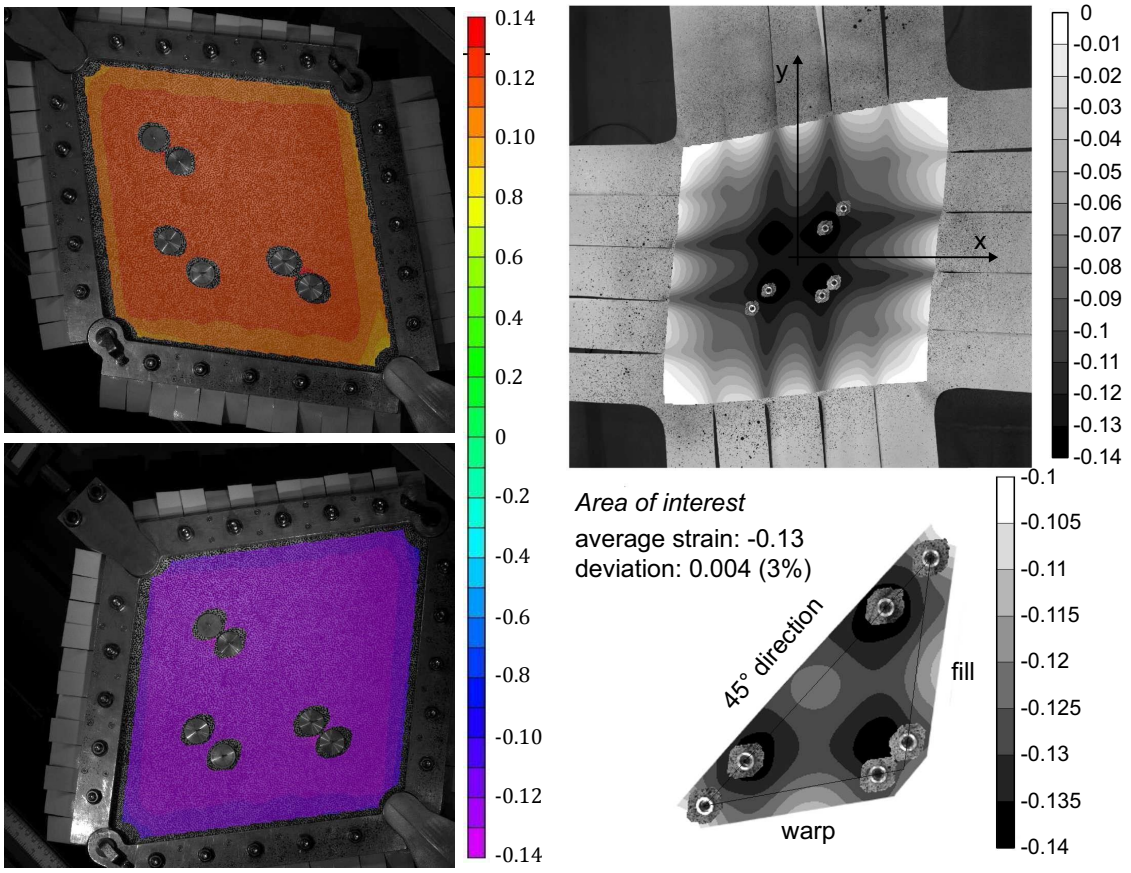

Fig 11. Shear strain ε_{xy} in the specimen (CMX220 at 3% UTS) obtained with Digital Image Correlation (DIC) (left). Contours intervals are the same as those used in the DIC images for the shear ramp method reproduced from Galliot and Luchsinger [25] (right). Each colour boundary indicates a difference in shear angle of 1.1°, γ = 15°.

Table 4.
Standard Deviation (SD) of shear strains

Mean ε_{xy}	Mean γ	SD ε_{xy}	% dev.
0.008	0.9	0.0004	5.0
0.024	2.8	0.0011	4.6
0.049	5.7	0.0023	4.7
0.073	8.4	0.0035	4.7
0.098	11.4	0.0047	4.8
0.123	14.2	0.0058	4.7

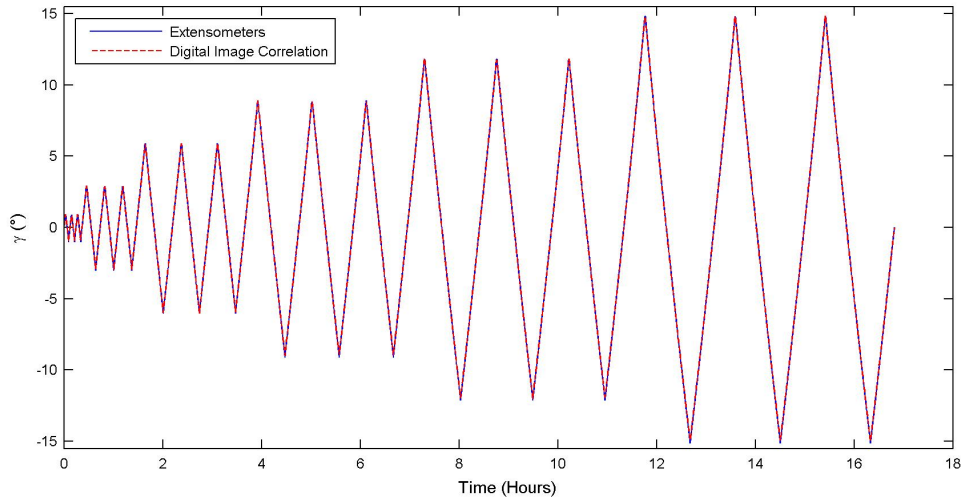

Fig 12. Comparison of the shear angle derived from the arrangement of linear extensometer and the DIC images (over the area of the extensometers). CMX220 at 3% UTS with modified shear profile shown.

4.2 Shear stress-strain cycles and calculation of the shear modulus

Plots of the test results (Fig. 13 and 14) separate sets of shear cycles by angle of shear deformation and fabric type and allow for a visual comparison of the shear behaviour between tests at different biaxial stresses. Each cycle can be seen to consist of a positive and negative half, with each half having a portion of loading (increasing absolute shear stress) and unloading (decreasing absolute shear stress). The cycles in Fig. 13 and 14 progress in the clockwise direction and each cycle set consists of 3 cycles (as previously shown in Fig. 7). Initially, values of shear stiffness were calculated as described in the MSAJ standard [13] (Fig. 12 and Table 5. The standard describes tip-to-tip measures of stiffness at +/- 1° of shear and is an average of the stiffnesses derived for the second and third cycles. The behaviour of the fabric during installation is captured during the initial cycle. Tip-to-tip stiffness is determined from the gradient of a line that connects the point of maximum shear stress-strain (the tip) of the positive half of a shear cycle with the point of maximum absolute shear stress-strain (the tip) of the negative half. Results show increasing shear stiffness with increased biaxial stress across the three fabrics tested. Accounting for shear at different biaxial stress states should be considered for accurate prediction of material behaviour, as differences of these magnitudes in shear stiffness have been shown to significantly impact the results of fabric structure analysis [4].

Elastic constants which approximately describe the in-plane biaxial behaviour of the SCC200 and CMX220 have previously been determined [37] and can be used to calculate ‘rule of thumb’

estimates of shear stiffness (shear stiffness = elastic modulus / 20) which would commonly be used industry [3]. , This gives shear stiffness values of 15-17kN/m for SCC200 and 43-58kN/m for CMX220 (the range of values reflects values calculated from the unequal warp and fill moduli). At 3% UTS (typical prestress) the rule-of-thumb measure for the SCC200 fabric is 22-31% less than the values measured using the picture frame, and for the CMZ220 fabric the rule of thumb value is 90-157% higher than that obtained through testing. These large differences suggest that the 'rule of thumb' can only provide a very approximate measure of shear stiffness and should be used with caution.

Tip-to-tip measures of shear stiffness effectively ignore the gradient of any individual part of the shear cycle. It can be seen from the plotted results (Fig. 13 and Fig. 14) that a line connecting the tips of each cycle, as described above, bares no similarity to the gradient of any part of the shear stress-strain cycles. Thus, it is suggested that an alternative means of approximating shear stiffness may offer a more accurate approximation of the shear stiffness by more closely matching the gradient exhibited by test data, or at least some part of it. It can be observed that a portion of each half of a cycle is substantially linear after an initial period of shear deformation that occurs either (i) after a change in the direction of shearing; or (ii) when shear deformation occurs at an angle that has not yet been prescribed by the test profile. It was noted that the latter observation is apparent only in the positive half of any cycle and that the linear parts of the positive and negative halves of all cycles are approximately parallel to each another. For the second and third cycles within each cycle set, the linear part is seen to extend for the loading portion of each half of the cycle. The gradient of this almost linear part of the curve provides a method for determining a value of shear stiffness that matches the fabric behaviour for a large portion of the curve, with arguably a closer fit to the test data than the tip-to-tip measures.

Alternative approximations of shear stiffness were calculated from the second and third cycles for both positive and negative halves of the cycles, along with comparative standard tip-to-tip measures, for each of the 13 cycle sets (Table 6). All tip-to-tip measures show increasing shear stiffness for all angles of shear deformation with increasing biaxial stress. However, the alternative approximations show no consistent discernable increase in shear stiffness with increasing biaxial stress for the parts of the cycles considered. The alternative measures of shear stiffness are similar for both the positive and negative halves of the shear stress-strain cycles. The rule-of-thumb measures compared to the alternative approximations for the positive loading portion of the shear cycles (again for the initial 1° cycles) are as follows: for the SCC200 fabric the rule-of-thumb measure is between 8.5% less and 3.7% more than the approximation of the test data; and for the CMX220 fabric the rule-of-thumb measure is 196-300% more than the approximation of the test result. Whilst the rule-of-thumb

measures for the SCC200 fabric is comparable to the alternative approximate measure, such closely matched results were not achieved from the CMX220 fabric.

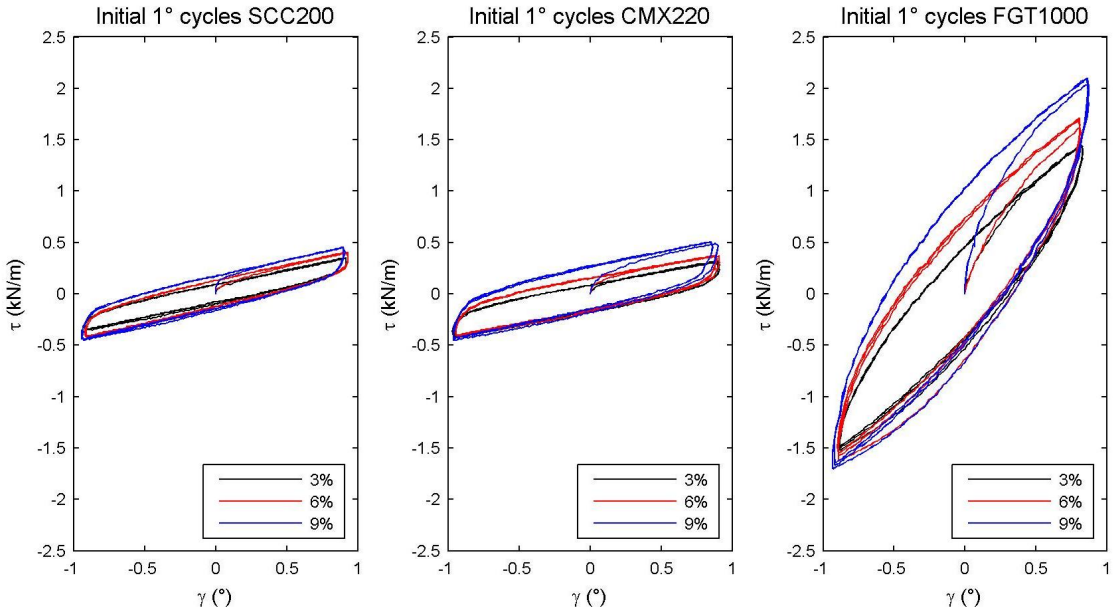

Fig. 13. Shear stress-strain plots for initial +/- 1° cycles. Results show increasing shear required to achieve 1° of deformation with increasing biaxial stress.

Table 5.
Shear modulus, G_{wf} – initial +/- 1° cycles

Fabric	Material	Shear stiffness, G_{wf} (kN/m)		
		3% UTS	6% UTS	9% UTS
SCC200	PET/PVC	21.8	25.7	28.0
CMX220	Glass/PVC	22.6	24.3	29.6
FGT1000	Glass/PTFE	99.2	109.9	120.5

G_{wf} - subscript wf denotes that shearing is aligned with the warp and fill directions

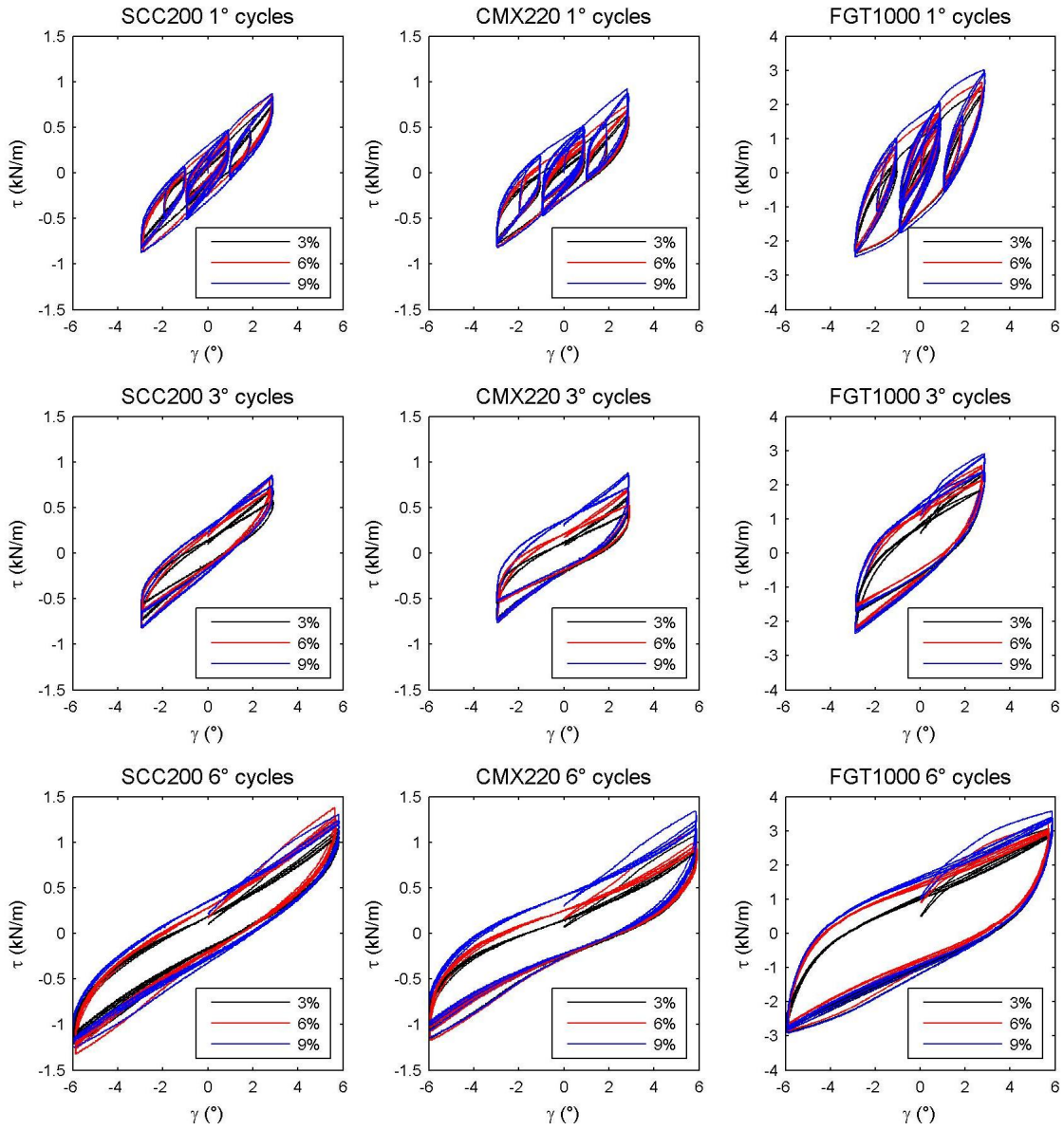

Fig 14. All shear cycles for all three materials tested separated into 1°, 3° and 6° cycle sets. The gradient of the curves, and consequently the shear modulus, decreases with increasing shear angle.

Table 6.
Shear modulus, G_{wf} – all cycle sets

		Shear modulus, G_{wf} (kN/m)								
		SCC200			CMX220			FGT1000		
Cycles	**% UTS**	+'ve curve	-'ve curve	Tip - Tip	+'ve curve	-'ve curve	Tip - Tip	+'ve curve	-'ve curve	Tip - Tip
1 (1°)	3%	16.4	16.4	21.8	14.5	14.5	22.6	66.8	63.2	99.2
	6%	16.8	18.0	25.7	14.2	14.5	24.3	67.0	62.6	109.9
	9%	17.6	18.0	28.0	16.1	16.2	29.6	67.3	63.7	120.5
2 (1°)	3%	18.1	12.9	21.8	16.6	11.2	22.7	56.2	51.4	89.6
	6%	18.3	15.3	26.0	16.3	11.2	24.6	55.2	57.6	98.3
	9%	17.0	15.1	27.0	18.0	12.9	30.1	58.0	57.4	109.4
3 (1°)	3%	13.0	14.8	19.2	10.9	12.6	19.5	52.7	56.0	85.6
	6%	14.7	16.7	23.9	11.5	14.1	23.0	53.2	58.4	98.0
	9%	15.2	16.7	26.1	12.9	15.1	27.9	53.8	58.6	106.2
4 (1°)	3%	12.2	16.4	21.0	10.0	15.5	21.6	42.9	51.4	82.0
	6%	13.9	19.1	25.8	11.2	16.5	25.4	46.3	53.8	95.2
	9%	13.5	16.7	26.4	13.1	17.4	29.1	48.8	55.1	102.9
5 (1°)	3%	12.5	12.8	17.8	10.6	10.3	18.0	51.7	49.4	79.3
	6%	13.8	14.9	22.3	10.7	10.9	20.7	48.8	50.0	88.1
	9%	14.4	14.8	24.5	12.0	11.9	25.3	51.2	51.0	97.4
6 (3°)	3%	12.1	12.3	14.2	10.3	10.6	13.1	29.4	28.3	46.3
	6%	13.0	13.4	16.5	10.2	11.1	14.2	26.2	29.4	47.8
	9%	11.5	11.9	16.3	10.6	11.2	15.8	27.9	29.0	51.6
7 (1°)	3%	11.9	12.1	17.1	10.0	10.1	17.2	47.4	46.6	74.3
	6%	13.2	14.4	21.7	10.0	10.6	20.0	44.9	46.9	82.5
	9%	14.2	14.3	23.8	11.3	11.5	24.4	47.3	48.5	91.6
8 (6°)	3%	10.1	10.2	11.4	8.6	9.0	10.1	18.7	16.5	28.3
	6%	10.8	10.8	12.8	8.0	8.9	10.4	16.2	17.9	28.8
	9%	8.9	8.9	11.9	8.5	8.7	11.3	17.5	17.1	30.6
9 (1°)	3%	9.9	10.1	15.1	8.4	8.1	14.6	38.8	36.2	62.8
	6%	11.1	12.6	19.2	7.9	8.1	17.2	37.3	36.3	69.5
	9%	11.8	12.2	21.2	9.3	8.9	21.5	39.1	37.0	77.6
10 (3°)	3%	8.8	8.9	11.2	6.9	6.9	9.7	22.3	21.0	36.5
	6%	9.8	9.9	13.4	6.7	7.1	10.6	20.0	21.3	37.4
	9%	9.1	9.2	13.7	7.4	7.2	12.3	21.3	20.8	40.6
11 (1°)	3%	10.1	10.3	15.2	8.5	8.6	14.6	39.5	37.2	62.4
	6%	11.4	12.2	19.4	8.1	8.5	17.4	37.5	37.9	69.1
	9%	12.5	12.6	21.6	9.6	9.2	21.7	38.9	38.3	76.8
12 (6°)	3%	9.6	9.9	10.7	8.2	8.5	9.3	19.3	17.6	27.3
	6%	10.4	10.6	12.2	7.3	8.3	9.4	16.6	19.7	27.8
	9%	8.9	9.2	11.6	7.9	8.2	10.4	18.2	18.8	29.5
13 (1°)	3%	9.5	9.6	14.6	8.2	7.6	14.1	37.5	34.3	60.6
	6%	10.7	11.6	18.7	7.6	7.9	16.8	35.8	35.0	67.1
	9%	11.5	11.9	20.8	9.0	8.6	21.2	37.6	35.2	74.2

G_{wf} - subscript wf denotes that shearing is aligned with the warp and fill directions

4.3 Shear deformation mechanisms

Shear deformation observed in coated woven fabrics is resisted by rotation at yarn intersections, yarn bending, shear of the coating and coating compaction. The observed increase in shear stiffness is likely to be the result of increased rotational friction at the yarn intersections, which is caused by an increase in out-of-plane contact forces. This is the only shear deformation mechanism that is likely to be affected by increasing levels of tension in the yarns. The differences observed between the cycles at increasing biaxial stress can be seen to arise during initial shear deformation. The phenomenon is best seen in the plots of the initial shear stress-strain behaviour to 1° (Fig. 13). Additional energy is required to overcome the frictional resistance in order to deform the fabric; the correlation between strain energy and biaxial stress is seen from the increasing area within the stress-strain curve (Figs. 13 and 14).

Increasing biaxial stress in the fabric will increase contact forces at the pins in the corners of the frame, with a corresponding increase in rotational friction of the hinges. The effect of frame friction with applied biaxial loading is difficult to isolate from the overall response of the frame plus fabric, and has not been considered in previous studies using picture frame shear testers. Biaxial load must be applied to the frame to simulate a shear test in a manner that does not introduce any shear resistance. Preliminary testing involved clamping two perpendicular strips of individual yarn bundles into the shear test frame, the yarn bundles having been first subjected to uniaxial loads (Fig. 15) which correspond to the biaxial load ratios considered in this study. A shear test was then conducted in the normal manner and the results compared to the results of the actual tests.

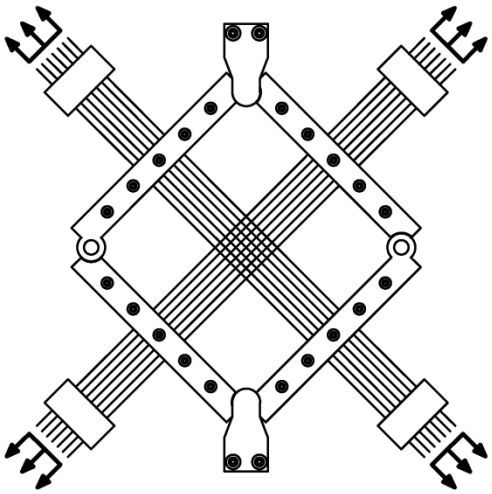

Fig 15. Preliminary testing to establish the influence of biaxial tension on the frictional resistance of the hinged frame.

This preliminary testing indicated that friction in the hinges of the frame accounts for approximately 10% of the total shear resistance recorded for any level of biaxial pretension. This means that the fabric is subjected to 90% of the expected level of shear stress. Further testing is required to accurately determine a 'stress reduction factor' that could be used in the calculation of shear moduli. The consistent and relatively small resistance of the hinges means that observations regarding the effect of changing levels of biaxial stress are valid.

4.4 Modelling shear stiffness

Any increase in shear stiffness with increasing biaxial stress has implications for the analysis methodology used for tensile fabric structures. Material properties used for analysis of tensile fabric structures are typically defined within a plane stress orthotropic framework, using elastic moduli and interaction terms [3] (Eq. 2).

$$\begin{Bmatrix} \varepsilon_w \\ \varepsilon_f \\ \varepsilon_{wf} \end{Bmatrix} = \begin{bmatrix} \frac{1}{E_w} & \frac{-v_{fw}}{E_f} & 0 \\ \frac{-v_{wf}}{E_w} & \frac{1}{E_f} & 0 \\ 0 & 0 & \frac{1}{G_{wf}} \end{bmatrix} \cdot \begin{Bmatrix} \sigma_w \\ \sigma_f \\ \sigma_{wf} \end{Bmatrix}$$

(Equation 2**)**

where ε = strain, σ = stress, E = direct stiffness G = shear stiffness and subscripts w and f denote warp and fill directions, respectively.

The plane stress framework allows complex non-linear behaviour to be approximated with linear parameters. This approach has the benefit of making fabric material behaviour compatible with commercial analysis software. The zero terms in the stiffness matrix indicate a lack of coupling between direct and shear behaviour, but the results the shear tests suggest that non-zero terms may be required to account for the influence of biaxial tension. However, due to the non-linear, hysteretic nature of the test results a different analysis framework may be more appropriate, as previously demonstrated for biaxial behaviour [9].

5 Conclusions

Comparing the available shear methodologies demonstrates the suitability of the picture frame test for characterising shear behaviour of architectural fabrics. The comparison also highlights tests which designers may wish to avoid, such as the KES-F test, the bias test and T-shaped specimen test, which cannot apply biaxial tension during shearing. A thorough appraisal of test methods is timely as development of a European standard for biaxial fabric testing and fabric structures design is underway; the CEN TC250 Working Group 5 has recently been established to write a standard for membrane structures for inclusion in Eurocode 10. In this context it would be useful to extend recent comparative biaxial testing studies [37, 39] to include shear test methods and protocols in multiple locations.

A robust shear test methodology has been demonstrated that subjects a test specimen to a known biaxial stress state, which is maintained whilst a homogenous shear deformation is applied. The homogeneity of the shear strain across the specimen makes determination of the shear stress in the fabric straightforward, however friction in the frame hinges does mean that a reduction factor is required to determine the shear force from the applied load. Given the difficulty of accurately determining the hinge friction with applied biaxial load, a pragmatic approach would be to minimise the friction in the frame to avoid the need for a reduction factor. For the frame presented above, replacement of the self-lubricating bushes with needle roller bearings could provide a significant reduction in friction and enable accurate determination of shear behaviour without the need for correction factors.

Shear *behaviour* is shown to change with increasing biaxial stress, with greater strain energy required to mobilise shear deformation in a highly tensioned fabric. Whether biaxial pretension affects the shear *stiffness* of the fabric depends on how the stiffness is evaluated from the non-linear, hysteretic shear response. The tip-to-tip value of shear stiffness varies with biaxial stress, but the effect on the gradient of the 'linear' part of the curve is minimal.

To include interaction of biaxial and shear stresses in the plane stress framework requires non-zero interaction terms, but further testing, and a consensus on how the shear stiffness should be calculated, would be required before values could be proposed. Given that the validity of using the plane stress framework to describe fabric behaviour is limited, it is proposed that further development should focus on methods that can fully capture the complex tensile and shear response of coated woven fabrics. One option currently being developed by the authors uses neural networks to relate stresses to strains with no assumptions about the form of the material response, with potential to incorporate stress history to capture hysteretic, visco-elastic behaviour.

Acknowledgements

Research funded by Architen-Landrell Associates (www.architen.com), Buro Happold (www.burohappold.com), the UK Engineering and Physical Sciences Research Council (www.epsrc.ac.uk), Serge Ferrari (en.sergeferrari.com), Tensys (www.tensys.com) and the Ministry of Economic Affairs R.O.C., with material contributions from F.I.T. Industrial Co. (www.fit-glassfiber.com.tw)

References

[1] Schock HJ. On The Structural Behavior and Material Characteristics of PTFE-Coated Glass-Fiber Fabric. Journal of Industrial Textiles. 1991;20(4):277-88.
[2] Gosling PD, Bridgens BN, Albrecht A, Alpermann H, Angeleri A, Barnes M, et al. Analysis and design of membrane structures: Results of a round robin exercise. Engineering Structures. 2013;48(0):313-28.
[3] Barnes M, Grundig L, Moncrieff E. Form-finding, load analysis and patterning. In: Foster B, Mollaert M, editors. European design guide for tensile surface structrues: TensiNet; 2004. p. 205-18.
[4] Bridgens B, Birchall M. Form and function: The significance of material properties in the design of tensile fabric structures. Engineering Structures. 2012;44(0):1-12.
[5] Berger H. Form and function of tensile structures for permanent buildings. Engineering Structures. 1999;21(8):669-79.
[6] Foster B, Mollaert M. Engineering fabric architecture. In: Foster B, Mollaert M, editors. European design guide for tensile surface structrues: TensiNet; 2004. p. 25-42.
[7] Grosberg P, Park BJ. Part V: The intial modulus and the frictional restraint in shearing of plain weave fabrics. Textile Research Journal 1966;36:420-31.
[8] Bridgens BN, Gosling PD, Birchall MJS. Membrane material behaviour: concepts, practice and developements. The Structural Engineer. 2004;82(14):28-33
[9] Gosling PD, Bridgens BN. Material Testing & Computational Mechanics - A New Philosophy For Architectural Fabrics. International Journal of Space Structures. 2008;23(4):215-32.
[10] Skelton J. Fundamentals of Fabric Shear. Textile Research Journal. 1976:862-9.
[11] Skelton J, Freeston JWD. Mechanics of elastic performance of textile materials. Part XIX: The shear behavior of fabrics under biaxial loads. Textile Research Journal. 1971;41(11):871-80.
[12] Pargana JB, Lloyd-Smith D, Izzuddin BA. Advanced material model for coated fabrics used in tensioned fabric structures. Engineering Structures. 2007;29(7):1323-36.
[13] MSAJ. Standard of the Membrane Structures Association of Japan. Testing method for in-plane shear stiffness of membrane materials. Membrane Structures Association of Japan; 1993.
[14] Cao J, Akkerman R, Boisse P, Chen J, Cheng HS, de Graaf EF, et al. Characterization of mechanical behavior of woven fabrics: Experimental methods and benchmark results. Composites Part A: Applied Science and Manufacturing. 2008;39(6):1037-53.
[15] Launay J, Hivet G, Duong AV, Boisse P. Experimental analysis of the influence of tensions on in plane shear behaviour of woven composite reinforcements. Composites Science and Technology. 2008;68(2):506-15.
[16] Lomov SV, Boisse P, Deluycker E, Morestin F, Vanclooster K, Vandepitte D, et al. Full-field strain measurements in textile deformability studies. Composites Part A: Applied Science and Manufacturing. 2008;39(8):1232-44.
[17] Zhu B, Yu TX, Tao XM. Large deformation and slippage mechanism of plain woven composite in bias extension. Composites Part A: Applied Science and Manufacturing. 2007;38(8):1821-8.
[18] Lebrun G, Bureau MN, Denault J. Evaluation of bias-extension and picture-frame test methods for the measurement of intraply shear properties of PP/glass commingled fabrics. Composite Structures. 2003;61(4):341-52.

[19] Page J, Wang J. Prediction of shear force and an analysis of yarn slippage for a plain-weave carbon fabric in a bias extension state. Composites Science and Technology. 2000;60(7):977-86.
[20] Bassett RJ, Postle R, Pan N. Experimental Methods for Measuring Fabric Mechanical Properties: A Review and Analysis. Textile Research Journal. 1999;69(11):866-75.
[21] Mohammed U, Lekakou C, Dong L, Bader MG. Shear deformation and micromechanics of woven fabrics. Composites Part A: Applied Science and Manufacturing. 2000;31(4):299-308.
[22] Vysochina K, Gabor A, Bigaud D, Ronel-Idrissi S. Identification of Shear Stiffness of Soft Orthotropic Textile Composites: Part I – Development of a Mixed Method for Shear Elastic Constant Identification. Journal of Industrial Textiles. 2005;35(2):137-55.
[23] Bögner-Balz H, Blum R. The Mechanical Behaviour of Coated Fabrics Used in Prestressing Textile Engineering Structures: Theory, Simulation and Numerical Analysis to Be Used in a FEM-Model. Journal of the International Association for Shell and Spatial Structures (J IASS). 2008;49(1):39-47.
[24] Jackson AL, Bridgens BN, Gosling PD. A new biaxial and shear test protocol for architectural fabrics. In: Domingo A, Lazaro C, editors. Evolution and Trends in Design, Analysis and Construction of Shell and Spatial Structures. Valencia: International Association for Shell and Spatial Structures (IASS); 2009. p. 2167-79.
[25] Galliot C, Luchsinger RH. The shear ramp: A new test method for the investigation of coated fabric shear behaviour – Part II: Experimental validation. Composites Part A: Applied Science and Manufacturing. 2010;41(12):1750-9.
[26] Galliot C, Luchsinger RH. The shear ramp: A new test method for the investigation of coated fabric shear behaviour – Part I: Theory. Composites Part A: Applied Science and Manufacturing. 2010;41(12):1743-9.
[27] Kawabata S. Nonlinear mechanics of woven and knitted materials. In: Chou T-W, Ko FK, editors. Textile structural composites. Amsterdam: Elsevier; 1989. p. 67-116.
[28] Lomov SV, Verpoest I, Barburski M, Laperre J. Carbon composites based on multiaxial multiply stitched preforms. Part 2. KES-F characterisation of the deformability of the preforms at low loads. Composites Part A: Applied Science and Manufacturing. 2003;34(4):359-70.
[29] Blum R, Bögner H, Némoz G. Testing Methods and Standards. In: Foster B, Mollaert M, editors. European Design Guide for Tensile Surface Structrues. Brussels: TensiNet; 2004. p. 293-322.
[30] Turner AW, Kabche JP, Peterson ML, Davids WG. Tension/torsion testing of inflatable fabric tubes. Experimental Techniques. 2008;32(2):47-52.
[31] Harrison P, Abdiwi F, Guo Z, Potluri P, Yu WR. Characterising the shear–tension coupling and wrinkling behaviour of woven engineering fabrics. Composites Part A: Applied Science and Manufacturing. 2012;43(6):903-14.
[32] Peng XQ, Cao J, Chen J, Xue P, Lussier DS, Liu L. Experimental and numerical analysis on normalization of picture frame tests for composite materials. Composites Science and Technology. 2004;64(1):11-21.
[33] Nguyen M, Herszberg I, Paton R. The shear properties of woven carbon fabric. Composite Structures. 1999;47(1-4):767-79.
[34] Farboodmanesh S, Chen J, Mead JL, White KD, Yesilalan HE, Laoulache R, et al. Effect of Coating Thickness and Penetration on Shear Behavior of Coated Fabrics. Journal of Elastomers and Plastics. 2005;37(3):197-227.
[35] Culpin MF. The shearing of fabrics: A novel approach. Journal of the Textile Institute. 1979;70(3):81-8.
[36] Peil KL, Barbero EJ, Sosa EM. Experimental Evaluation of Shear Strength of Woven Webbings. SAMPE 2012. Baltimore2012.
[37] Bridgens BN, Gosling PD, Jou G-T, Hsu X-Y. Inter-laboratory comparison of biaxial tests for architectural textiles. Journal of the Textile Institute. 2012;103(7):706-18.
[38] Colman AG, Bridgens BN, Gosling PD. A picture frame shear test methodology to determine accurate shear properties of architectural fabrics. TensiNet Symposium: [Re}Thinking lightweight structures. Istanbul, Turkey: TensiNet; 2013.
[39] Beccarelli P, Bridgens B, Galliot C, Gosling P, Stimpfle B, Zanelli A. Round-robin biaxial tensile testing of architectural coated fabrics Proceedings of the International Symposia IABSE-IASS 2011:Taller, Longer, Lighter. London2011.